

RESEARCH

Open Access



Activation of embryonic/germ cell-like axis links poor outcomes of gliomas

Zhan Ma^{1,2†}, Fengyu Zhang^{1†}, Ji Xiong^{3†}, Haishi Zhang^{4†}, Hui-Kuan Lin⁵ and Chunfang Liu^{1*}

Abstract

Background: It is unclear which core events drive the malignant progression of gliomas. Earlier studies have revealed that the embryonic stem (ES) cell/early PGC state is associated with tumorigenicity. This study was designed to investigate the role of ES/PGC state in poor outcomes of gliomas.

Methods: Crispr-Cas9 technology, RT-PCR and animal experiments were used to investigate whether PGC-like cell formation play crucial roles in the tumorigenicity of human glioma cells. Bioinformatic analysis was used to address the link between ES/PGC developmental axis and glioma overall outcomes.

Results: Here, our findings showed that germ cell-like cells were present in human gliomas and cultured glioma cells and that the formation of germ cell-like cells was essential for glioma tumours. Bioinformatic analysis showed that the mRNA levels of genes related to embryonic/germ cell development could be detected in most gliomas. Our findings showed that the activation of genes related to reprogramming or the germ cell-like state alone seemed to be insufficient to lead to a malignant prognosis, whereas increased mRNA levels of genes related to the activation of the embryonic/germ cell-like cycle (somatic PGC-EGC-like cycle and somatic parthenogenetic embryo-like cycle) were positively correlated with malignant prognoses and poor clinical outcomes of gliomas. Genes related to the embryonic/germ cell cycle alone or in combination with the WHO grade or 1p19q codeletion status could be used to subdivide gliomas with distinct clinical behaviours.

Conclusion: Together, our findings indicated that a crucial role of germ cell-like cell formation in glioma initiation as well as activation of genes related with the parthenogenetic embryo-like cycle and PGC-EGC-like cycle link to the malignant prognosis and poor outcomes of gliomas, which might provide a novel way to better understand the nature of and develop targeted therapies for gliomas as well as important markers for predicting clinical outcomes in gliomas.

Keywords: Gametogenesis hypothesis of tumours, Glioma prognosis, Embryonic/germ cell-like cycle, Primordial germ cell-like tumor cells, Markers for poor outcomes of glioma patients

Introduction

Despite differences in their tissues of origin and genetic backgrounds, many tumours exhibit common phenotypes, such as high embryonic/germ cell traits, which is accounted for in the embryo/gametogenesis-related hypothesis of tumours proposed by Müller (1838), Langenbeck (1840) and Beard (1902) and extended by Old (2001) [1–5]. This hypothesis postulated that tumours arise from germ cells or reactivation of the germ cell programme in somatic tissues. Earlier studies have revealed

[†]Zhan Ma, Fengyu Zhang, Ji Xiong and Haishi Zhang contributed equally to this work

*Correspondence: chunfang_liu@fudan.edu.cn

¹ Department of Laboratory Medicine, Shanghai Medical College, Huashan Hospital, Fudan University, Shanghai 200040, China
Full list of author information is available at the end of the article



that tumorigenicity is an inherent feature of the embryonic stem (ES) cell/early primordial germ cell (PGC) state, including early PGCs, implantation embryos, parthenogenetic oocytes, embryonal carcinoma (EC) cells, embryonic stem (ES) cells, embryonic germ cells (EGCs) and induced pluripotent stem (iPS) cells [6–11], raising the possibility that re-obtaining the ES/early PGC state may be one of the driving events in the malignant behaviours of somatic tumours.

An increasing number of studies have revealed that embryonic/germ cell-specific genes play crucial roles in tumorigenicity, metastasis and therapy resistance [12–25]. Notably, it has been shown that knockout of those genes related to germ cell development fully inhibits brain tumour formation in *Drosophila* [26], and no melanoma initiation occurs before the reactivation of genes related to embryonic development in a zebrafish model [27]. Our previous studies showed that embryonic/germ cell-like tumour cells were found in various types of tumours, played important roles in tumour growth, liver metastasis and drug resistance; and exhibited an independent life cycle [19–21, 28–31]. We also showed that the formation of embryonic/germ cell-like tumour cells was induced by either p53 deficiency or a chemical carcinogen (3-methylcholanthrene, 3-MCA) [20, 28]. In essence, PGCs give rise to sperm or oocytes and then return to the embryonic state via fertilization or parthenogenesis. However, PGCs can also return to the embryonic state via PGC-EGC conversion under some conditions, such as *PTEN/TP53/SOX17* deficiency [9, 32, 33]. Therefore, we postulated that the acquisition and maintenance of the ES/early PGC state via activation of the embryonic/germ cell-like developmental axis might be linked to the core malignant behaviours of somatic tumours through somatic cell-ESC/PGC-(post-migratory PGC)-EGC-somatic cell-like conversion (which we named the somatic PGC-EGC/ES-like cycle) and/or somatic tumour cell-ESC/PGC-(post-migratory PGC)-oocyte-parthenogenetic embryo-somatic tumour cell conversion (which we named the somatic parthenogenetic embryo-like cycle) [20] (Fig. 1A). Here, our findings showed that activation of the embryonic/germ cell-like development axis was essential in the malignant progression of gliomas and that related genes could be used as important markers to predict clinical outcomes in gliomas.

Methods

Cell culture

U251, LN229 and A172^{wt} cells were obtained from ATCC. A172^{mut} cells were derived from A172^{wt} cells after treatment with a chemical carcinogen (3-methylcholanthrene, 3-MCA). All cells were cultured in high-glucose

Dulbecco's modified Eagle's medium (DMEM, HyClone) with 10% foetal bovine serum (FBS; Sigma) and 1% L-glutamine and were maintained at 37 °C with 5% CO₂.

Single cell cloning

U251 or A172^{mut} cells were plated in 96-well plates by the limited dilution method and incubated at 37 °C with 5% CO₂ for proliferation. Wells with single cells were selected and then treated with AP staining after culturing for 3 weeks. The efficiency of generating PGC-like cells was counted in the single clones.

Alkaline phosphatase staining

Cultured cells were fixed with 4% paraformaldehyde in PBS for 4 min, washed twice with a Tris-HCl (pH=8.6) buffer solution and then incubated with AP substrate (Vector laboratory) for 40 min at room temperature.

Real-time PCR analysis

RNA was isolated from cultured cells by Trizol reagent (Invitrogen) and then converted to cDNA by reverse transcription using a reverse transcription kit (Invitrogen). Real-time PCR analysis was performed with a SYBR Green PCR Master Mix Kit (Applied Biosystems) according to the manufacturer's instructions.

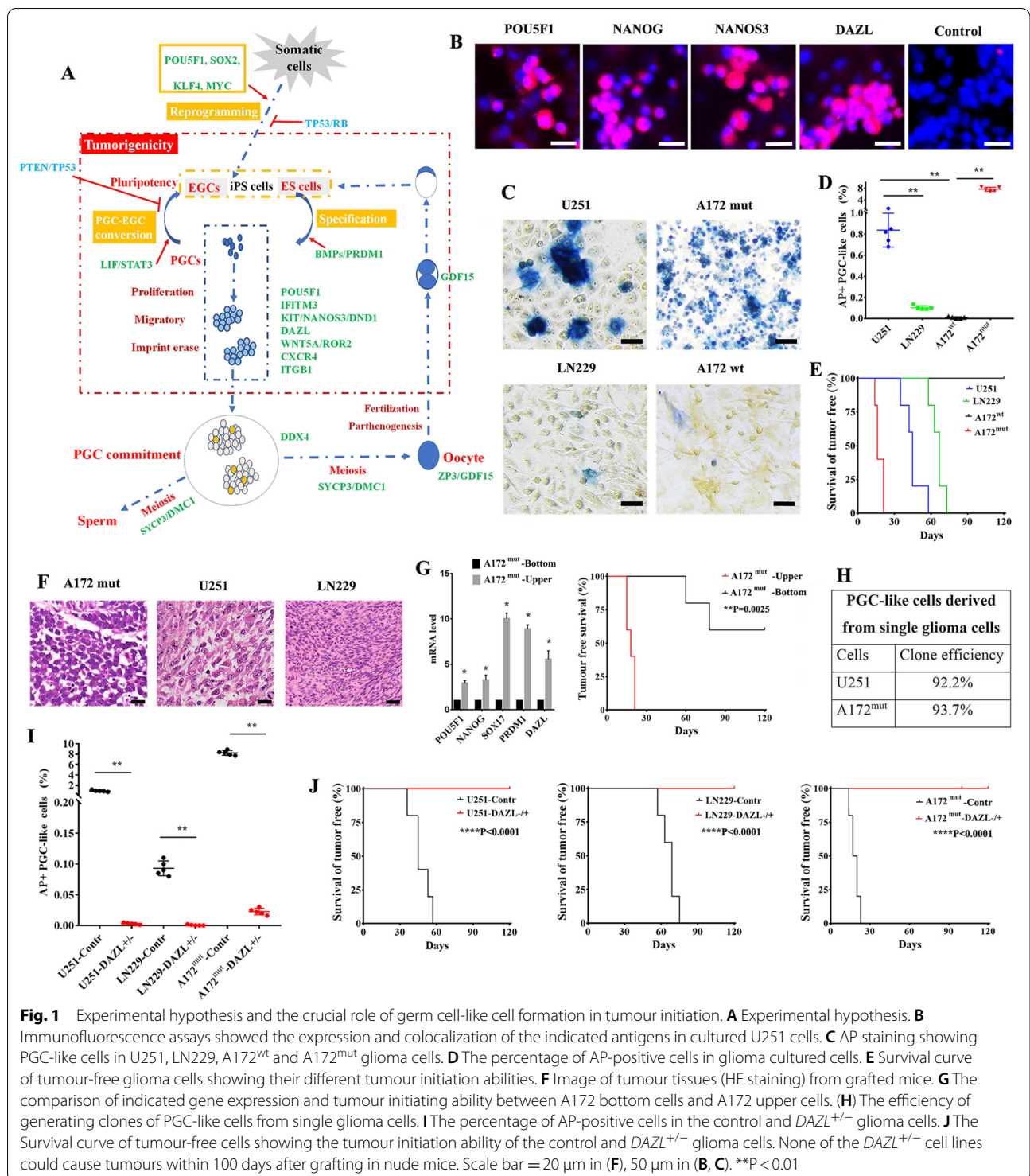
Animal experiments

All animal protocols were carried out in accordance with ARRIVE guidelines.

To compare tumorigenicity, the U251, LN229, A172^{wt} and A172^{mut} cells, U251-*DAZL*^{+/-}, LN229-*DAZL*^{+/-}, A172^{mut}-*DAZL*^{+/-} cells, U251-guide, LN229-guide and A172^{mut}-guide (1.5×10^5 cells/mice) were subcutaneously injected into female nude mice (n=5, age 6 weeks, body weight 20–22 g) respectively. The time of tumour initiation was recorded every day. Five mice were raised in a cage under specific pathogen-free conditions and a 12-h light/dark cycle at 23 ± 2 °C and $60 \pm 10\%$ humidity, and standard food and water were freely available. At the end of the experiment, the mice were euthanized via exposure to a gradually increasing concentration of carbon dioxide gas in accordance to ARRIVE guidelines and then resected the subcutaneous tumors which were then fixed in 4% formaldehyde for pathological analysis. A P-value < 0.05 was considered to be significant.

Immunocytochemistry

Cells were cultured on coverslips, fixed with 4% paraformaldehyde and then blocked in PBS with 5% BSA and 0.05% Triton-X-100. Cells or tissue sections were incubated overnight at 4 °C with various primary antibodies, including anti-POU5F1 (ab184665, Abcam), anti-Sox2 (MAB2018R-100, R&D), anti-Nanog (NB100-58842,



Novus Biologicals), anti-Nanos3 (ab70001, Abcam), anti-DDX4 (ab27591, Abcam), SCP3 (ab 15,093, Abcam) or anti-DAZL (NB100-2437, Novus biologicals). Next, the cells were stained with Cy3 fluorescent dye-conjugated secondary antibodies (Jackson) and

4,6-diamidino-2-phenylindole (DAPI; Invitrogen), while the tissue sections were stained with haematoxylin. The cells just were stained with Cy3 fluorescent dye-conjugated secondary antibodies (Jackson) and 4,6-diamidino-2-phenylindole (DAPI; Invitrogen) as control.

DAZL deletion

The CRISPR/Cas9 and sgRNA-RFP plasmids were provided by Addgene and Sigma, respectively [24]. The *DAZL*-sgRNAs sequences are: GAAGCTTCTTTGCTA GATATGG (Additional file 1: Table S1). The guide empty vector was used as the blank control (Sigma). To delete *DAZL* in U251, LN229 and A172^{mut} cells, we transfected glioma cells simultaneously with the CRISPR/Cas9 vector and guide RNAs (gRNAs) as described previously [21, 24]. Guide gene was used as a knockout control. Two days post transfection, the treated glioma cells were selected with 4 µg/ml of blasticidin or 5 µg/ml of puromycin for 5 days. Single cells were then isolated from the selected cells by dilution and clonally expanded. Single clone cells with *DAZL* deletion were selected by gene sequencing. The clone cells with *DAZL* frameshift mutation were *DAZL*^{+/-} (Additional file 1: Fig. S1). We got 9 *DAZL*^{+/-} U251 cells, 3 *DAZL*^{+/-} LN229 cells and 7 *DAZL*^{+/-} A172^{mut} cells.

Tissue specimens

Glioma tissues were obtained from 38 patients with gliomas, including 20 grade IV gliomas, 8 grade III gliomas and 10 grade II gliomas. All patients underwent curative resection at Huashan Hospital of Fudan University from 2011 to 2013. Glioma tissues were stained with hematoxylin eosin (HE) or antibody.

Data of the CGGA database

Data from the Cancer Genome Atlas (TCGA), the Genotype-Tissue Expression (GTEx) and the Chinese Glioma Genome Atlas (CGGA) (<http://cgga.org.cn/index.jsp>) were used to confirm our concept. The Data from the Cancer Genome Atlas (TCGA) and the Genotype-Tissue Expression (GTEx) were analysed using the <http://gepia2.cancer-pku.cn/#analysis>. The WEsseq_286 dataset was used to analyse the genetic mutations. The methyl_159 dataset was used to analyse the methylation status of various genes. The mRNAseq_325 and mRNAseq_693 datasets (Additional file 1: Table S2) were used to analyse the mRNA levels of various genes as well as to investigate whether the mRNA level was associated with the pathologic grades or outcomes of gliomas. The mRNA-array_301 dataset was used to analyse the mRNA level of *DAZL* in gliomas and its link to the pathologic grades and outcomes of gliomas. Data without overall survival information were deleted. Detailed information on the datasets for mRNA sequencing is provided in Additional file 1: Table S2.

Statistical analysis

Kaplan–Meier curves were used to assess overall survival for each of the genes and test groups. Unpaired t

test with Welch's correction and Mann Whitney test were used to analyse the difference of gene expression between distinct groups.

Results

A crucial role of germ cell-like cell formation in tumour initiation

PGC-like cells were frequently observed in U251 and A172 mutant (A172^{mut}) glioma cell cultures but were barely observed in LN229 and A172 wild-type (A172^{wt}) glioma cell cultures (Fig. 1B–D, Additional file 1: Fig. S2A, B). We found that germ cell-like cell formation was positively correlated with tumour initiation in glioma cells, including U251, LN229, A172^{wt} and A172^{mut} cells (Fig. 1D and E). Notably, A172^{wt} cells without germ cell-like cell properties failed to form tumour within 120 days after grafting in nude mice. However, A172^{mut} cells that reobtained germ cell-like properties after treatment with a chemical carcinogen (3-methylcholanthrene, 3-MCA) gave rise to tumours within 2 weeks of grafting in nude mice (Fig. 1E). Interestingly, tumour tissues derived from A172^{mut} cells were teratocarcinomas (Fig. 1F), which provided strong support for the presence of germ cell-like cells since teratocarcinomas are thought to originate from germ cells [2, 5]. Germ cell-like tumour cells often grow above somatic tumour cells and can be easily separated from somatic tumour cells in vitro. We separated the upper cultures, which were enriched with PGC-like cells, from the bottom cultures, which contained a small proportion of PGC-like cells in A172^{mut} cells, by shaking the flask rigorously. RT-PCR data showed that the expression of genes related to germ cells was much higher in the upper cells than in the bottom cells in A172^{mut} cultures (Fig. 1G). Compared to the bottom cells, the upper cells in A172^{mut} cultures showed increased tumour initiation abilities after injection into nude mice (Fig. 1G). Notably, SOX17 which links to the PGC state of human were reactivated in the upper cells of A172^{mut} cultures and expressed highly versus SOX2 which links to ES state of human (Additional file 1: Fig. S2C). After culture, most single U251 and A172^{mut} cells generated clones containing PGC-like cells, indicating that PGC-like cells could be derived from somatic glioma cells (Fig. 1H).

We then investigated the relationship between germ cell formation and tumour initiation by deleting *DAZL*, which plays a crucial role in germ cell development from PGC specification, PGC fate determination to PGC further mature [34–36], with CRISPR-Cas9 technology. Since *DAZL*^{-/-} glioma cells were not viable in culture possibly attributed to a crucial role of *DAZL* or germ cell fate in immortality of tumour cells, U251-*DAZL*^{+/-}, LN229-*DAZL*^{+/-} and A172^{mut}-*DAZL*^{+/-} cells were studied (Additional file 1: Table S2). Our earlier study revealed

that knockdown of *DAZL* inhibited tumour formation and increased the therapeutic sensitivity of cultured human glioma cells [24]. In this study, we further revealed that knockdown of *DAZL* greatly impaired germ cell formation and tumour initiation in U251, LN229 and A172^{mut} cells (Fig. 1I and J). These findings showed that activation of PGC-like cell formation from somatic tumour cells was essential in the initiation of glioma cell tumours, leading to tumorigenicity in new sites. Thus, activation of the PGC-like state might be necessary for a more aggressive stage of gliomas.

Genetic and epigenetic changes in genes related to embryonic/germ cell development in gliomas

PGC specification arises from ES cells [36–38], and findings in iPS cells highlight the possibility of somatic cell reprogramming [11]. This means that if a PGC-like fate truly occurs in gliomas, at least two key events are possibly involved: reprogramming and PGC specification (Fig. 1A). Therefore, we investigated whether the genes related to reprogramming, PGC specification and PGC development (including conversion of PGCs into EGCs and oogenesis from PGCs) were activated in gliomas and linked to the malignant prognosis of gliomas (Fig. 1A). The defined gene groups included those involved in reprogramming (inhibition: *TP53*; promotion: *POU5F1*, *SOX2*, *MYC*, *KLF4*), pluripotency (*POU5F1*, *SOX2*, *MYC*, *KLF4*, *NOTCH1*), induction of ES-PGC conversion by microenvironment (*BMP2*, *BMP4*, *BMP8B*, *LIF*), PGC specification (*POU5F1*, *PRDM1*, *SOX17*, *ACVRL1*, *IFITM3*), PGC fate maintenance (*SOX17*, *PRDM1*, *KIT*, *Nanos3*, *DND1*), PGC survival (*DAZL*, *DDX4*), proliferation/migration/survival (*ITGB1*, *CXCR4*, *WNT5A*, *ROR2*), meiosis (*SYCP3*, *DMC1*), PGC-EGC conversion (inhibition: *TP53*, *PTEN*, *BMP2*, *BMP4*, *SOX17*; promotion: *LIF*, *STAT3*), oocytes (*ZP3*, *GDF15*) as well as early embryos (*GDF15*) [11, 33, 36, 37, 39–44].

To validate our hypothesis, Chinese Glioblastoma Genome Atlas (CGGA) data were analysed. Since tumorigenicity is thought to be the outcome of a series of genetic and epigenetic changes, we first investigated whether genetic and epigenetic changes in the gene groups were present in human gliomas. The whole-exome sequencing results of gliomas from the CGGA database showed that there were few or no genetic changes among a series of core genes and signalling pathways related to the embryonic/germ cell developmental axis in human gliomas (Fig. 2A). Additionally, the methylation analysis results revealed that most of the genes showed reduced levels of

methylation (Fig. 2C). Of note, *TP53* (46%), which inhibits reprogramming, PGC-EGC conversion and oocyte development [20, 36, 45, 46]; *PTEN* (7%), which strongly inhibits PGC-EGC conversion [9, 36]; and *NOTCH1* (8%), which promotes pluripotency [36], were frequently detected among the genetic changes (Fig. 2A). *TP53* and *PTEN* mutations were correlated with poor outcomes, while *NOTCH1* mutations were associated with improved outcomes (Fig. 2B). The data indicated that epigenetic changes but not genetic changes, occurred in most of the core genes related to the embryonic/germ cell developmental axis in human gliomas, while the suppressor genes associated with reprogramming or PGC-EGC conversion frequently lost in gliomas with poor outcomes. Moreover, the reduced levels of methylation in the gene groups supported the activation of genes in gliomas. It is possible that the obtaining of embryonic/germ cell-like traits is activated by methylation changes of embryonic/germ cell-related genes.

Links of the embryonic/germ cell development-like axis to a malignant prognosis

Gliomas are pathologically classified as glioblastomas (GBM, grade WHO IV) and lower-grade gliomas (LGG, grades WHO II and WHO III) and have distinct malignant stages and outcomes [47]. We analysed the TCGA and GTEx dataset to compare the expression of several genes related with embryonic/germ cell development between gliomas and normal brain tissues. Compared to normal brain tissues, the mRNA level of *SOX2*, *MYC*, *NOTCH1*, *STAT3*, *BMP2*, *ACVRL1*, *ITGB1*, *WNT5A*, *CXCR4* and *ZP3* increased significantly in both GBM and LGG as well as the mRNA levels of *LIF*, *PRDM1*, *IFITM3* and *GDF15* increased significantly in GBM but not in LGG (Additional file 1: Fig. S3). However, there was no significant differentiation in the mRNA levels of *BMP4*, *BMP8B*, *SOX17*, *KIT*, *NANOS3*, *DND1*, *DAZL*, *DDX4*, *ROR2*, *SYCP3* and *DMC1* between gliomas and normal brain tissues (not shown). To further determine whether the gene groups were activated in gliomas and linked to pathologic classification, malignant prognosis and clinical outcomes, we analysed the mRNA sequencing results of gliomas from the CGGA database. The data showed that IPS reprogramming factors and pluripotency-related genes (*POU5F1*, *SOX2*, *KLF4*, *MYC* and *NOTCH1*) were detected in almost all histologic types and grades of gliomas (Fig. 3A, B, and Additional file 1: Fig. S4A, S5A, Table S3–S5). While the mRNA levels of genes related to pluripotency (*SOX2*, *KLF4*, *MYC* and *NOTCH1*) were

(See figure on next page.)

Fig. 2 Genetic and epigenetic changes in genes related to embryonic/germ cell development. **A** Whole-exome sequencing data showing the mutational landscape of various genes (the results of *POU5F1*, *SOX2*, *STAT3*, *LIF*, *ITGB1*, *CXCR4*, *WNT5A*, *SYCP3* and *DMC1* were not found in the CGGA database). **B** Overall survival (OS) curve showing the association of DNA changes in *TP53*, *PTEN* and *NOTCH1* with the outcomes of gliomas. **C** Methylation data showing the methylation state of various genes

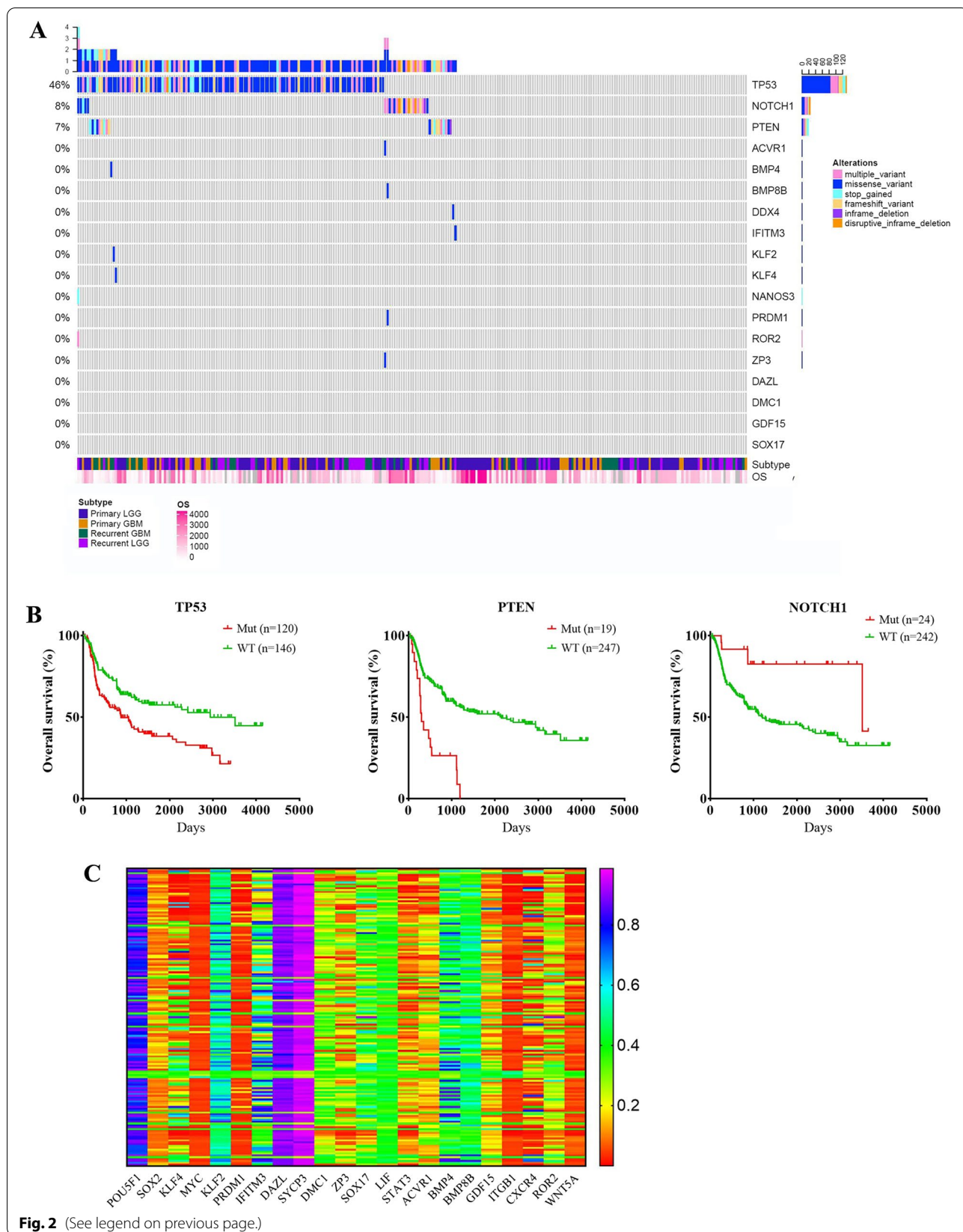


Fig. 2 (See legend on previous page.)

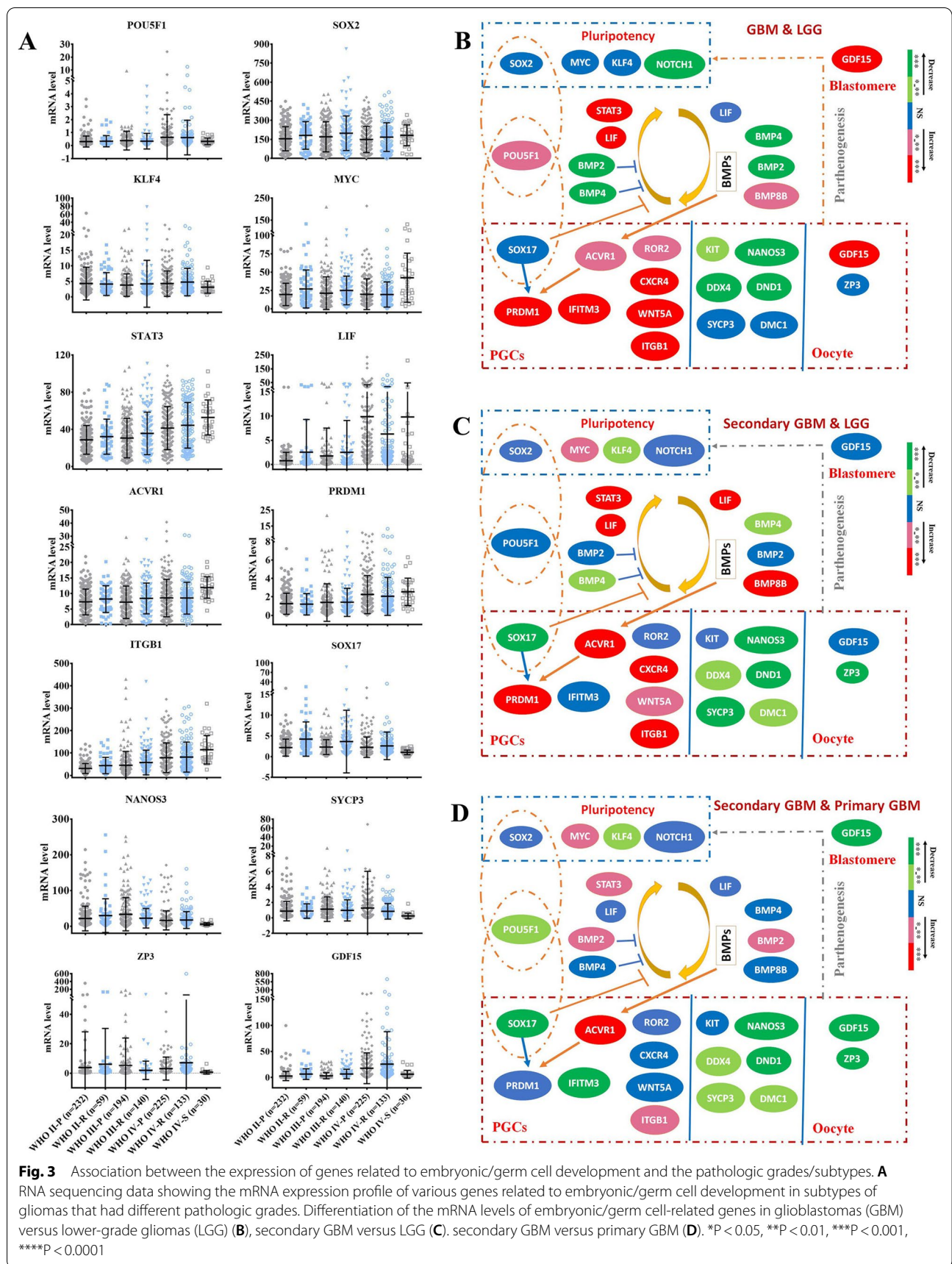
not obviously correlated with the clinical glioma grade or outcome, the mRNA level of *POU5F1*, which also plays a crucial role in PGC specification, was often linked to a higher glioma grade and poor outcome (Fig. 3A, B, 4A, C, D and Additional file 1: Fig. S6A, Table S3–S5). These findings revealed that the activation of reprogramming-related genes was commonly seen even in low-grade gliomas; however, it might be insufficient to lead to a malignant prognosis.

As expected, the mRNA sequencing results of gliomas from the CGGA database showed that the mRNA levels of various genes related to germ cell development were also enriched in some gliomas, including *LIF*, *PRDM1*, *BMP2*, *BMP4*, *BMP8*, *ACVR1*, *IFITM3*, *ITGB1*, *CXCR4*, *WNT5A*, *ROR2*, *ZP3*, *GDF15*, *SOX17*, *DAZL*, *DDX4*, *SYCP3* and *DMC1* (Fig. 3A, and Additional file 1: Fig. S4, S5B, S5C, Table S3, S4). The mRNA levels of *PRDM1*, a core germ cell specification gene, as well as its core upstream gene *ACVR1* and downstream gene *IFITM3* were totally associated with advanced pathologic grades and poor outcomes (Figs. 3B and 4B–D, and Additional file 1: Fig. S5B, S6A, Table S3–S5). High mRNA levels of genes related to PGC proliferation/survival/migration (*ITGB1*, *CXCR4*, *WNT5A* and *ROR2*), ES-PGC conversion (*BMP8B* and *LIF*), PGC-EGC conversion (*LIF* and *STAT3*), PGC survival (*DAZL*) and oocytes/early embryos (*GDF15*) also showed total correlations with an advanced pathologic grade and poor overall survival of patients (Figs. 3B and 4B–D, and Additional file 1: Fig. S5B, S6A, Table S3–S5). Notably, *POU5F1* partners with *SOX2* in human ES cells and partners with *SOX17* in human PGCs [33, 38]. Although the mRNA levels of *SOX17*, a core germ cell specification gene [38], were enriched in some gliomas, they did not show obvious correlations with advanced pathologic grades and poor outcomes (Figs. 3B and D and 4C, D and Additional file 1: Fig. S5B, S6A, Table S3–S5), likely because *SOX17* also inhibits PGC-EGC reprogramming [33]. The mRNA level of gene related with later meiosis (*DMC1*) was slightly associated with poor overall survival (Fig. 4C, D and Additional file 1: Fig. S5B, S6A, Table S5). The mRNA levels of genes related to the activation of ES-PGC conversion but inhibition of PGC-EGC conversion (*BMP2* and *BMP4*), late PGCs (*DDX4*), meiosis entry (*SYCP3*) as well as genes related to PGC fate determination (*KIT*, *NANOS3* and *DND1*) showed no or negative correlations with advanced pathologic grades and poor outcomes (Figs. 3B and 4C and Additional file 1: Fig. S5B, S6A, Table S3–S5). These data suggest that tumour cells arrested in the germ cell-like developmental stage (not early PGC-like stage) and that lost the ability to return to the embryonic cell-like state might not lead to a malignant prognosis of gliomas. Compared with LGG,

GBM showed higher expression of *POU5F1*, *PRDM1*, *BMP8B*, *LIF*, *STAT3*, *ACVR1*, *IFITM3*, *ITGB1*, *CXCR4*, *WNT5A*, *ROR2* and *GDF15* (Fig. 3A, B, and Additional file 1: Fig. S2A, Table S4), indicating that both the activation of the PGC-like state and the return of germ cells to the embryo-like state were essential in the malignant behaviours of some gliomas via somatic parthenogenetic embryo-like cycle and/or somatic PGC-EGC/ES-like cycle. Compared with LGG, secondary GBM arising from LGG [48] showed higher expression of *PRDM1*, *BMP8B*, *ACVR1*, *LIF*, *STAT3*, *ITGB1*, *WNT5A*, *CXCR4*, *MYC* but decreased expression of genes related to germ cell fate, including *Nanos3*, *DND1*, *BMP2*, *BMP4*, *SOX17*, *DDX4*, *SYCP3*, *DMC1* and *ZP3* (Fig. 3A, C, and Additional file 1: Fig. S4A, Table S4), indicating that the PGC-EGC/ES-like conversion pathway rather than the mature development pathway might be activated in secondary GBM and that the activation of PGC-EGC/ES-like cycle was linked to the malignant prognosis of LGG. Compared with primary GBM, secondary GBM showed higher expression of *ITGB1*, *ACVR1*, *MYC*, *STAT3* and *BMP2* but significantly decreased expression of genes related to germ cell mature (*Nanos3*, *DND1*, *DDX4*, *SOX17*, *SYCP3*, *DMC1*, *ZP3* and *GDF15*) and genes related to inhibition of PGC-EGC conversion (*BMP4* and *SOX17*) (Fig. 3A, D, and Additional file 1: Fig. S4A, Table S3), further indicating that the activation of PGC-EGC/ES-like conversion was one of driving events to malignant prognosis of gliomas. In addition, the decreased expression of genes related to germ cell development was accompanied by the decreased expression of *GDF15*, consistent with the fact that activation of gene *GDF15* links to the oocyte/early embryo-like state (Fig. 3A, D, and Additional file 1: Table S3). Collectively, these findings indicated that the genes related to the activation of the parthenogenetic embryo-like cycle and activation of the PGC-EGC-like cycle were both linked to poor patient outcomes, which might represent two pathways that drive the malignant prognosis of gliomas.

Inhibition of embryonic/germ cell cycle-related gene expression among gliomas with 1p19q codeletion

LGG have wide survival ranges, from 1 to 15 years, and distinct therapeutic sensitivities [47]. LGG with deletion of chromosome arms 1p and 19q (1p19q codeletion) are often associated with impressive therapeutic sensitivities and favourable clinical outcomes [47]. Consequently, we determined whether genes related to the embryonic/germ cell developmental axis were inhibited in glioma samples with 1p19q codeletion. The combined mRNA sequencing data from the 325 and 694 datasets of CGGA showed that the mRNA levels of *POU5F1*, *LIF*, *BMP8B*, *ROR2*, *CXCR4*, *IFITM3*, *ITGB1* and *GDF15*



were extremely low in almost all glioma samples with 1p19q codeletion (1p19q-codel) compared to glioma samples without 1p19q codeletion (1p19q-noncodel) (Fig. 5A–C, and Additional file 1: Table S6). Overall, the mRNA levels of *ACVR1*, *STAT3*, *WNT5A*, *KLF4* and *DMC1* were obviously decreased in glioma samples with 1p19q codeletion compared to those in glioma samples without 1p19q codeletion (Fig. 5A–C, and Additional file 1: Fig. S7, Table S6). However, 1p19q codeletion did not inhibit the mRNA levels of *SOX2*, *SOX17*, *SYCP3*, *MYC*, *ZP3*, *NOTCH1*, *DDX4*, *KIT*, *NANOS3*, *DND1*, *BMP2* and *BMP4* (Fig. 5A–C, and Additional file 1: Fig. S7, Table S6). These findings indicated that 1p19q codeletion robustly inhibited genes involved in promoting the embryonic/germ cell cycle.

Clinical significance of embryonic/germ cell cycle-related molecular groups among gliomas

Histopathological classification is often performed in gliomas; however, this method is not sufficient to predict clinical outcomes [47]. Consequently, we performed an analysis of the molecular group related to the embryonic/germ cell cycle (including *LIE*, *STAT3*, *PRDM1*, *IFITM3*, *ACVR1*, *CXCR4*, *WNT5A*, *ROR2*, *ITGB1*, *POU5F1*, *GDF15* and *BMP8B*) (Additional file 1: Table S7) to determine whether we could identify glioma outcomes more accurately based on the germ cell-related molecular group than based on the histologic class. The combined mRNA sequencing data of 325 and 694 CGGA datasets showed that patients with higher expression of genes in the molecular group had much poorer overall survival than patients with lower expression of genes in the gene groups (Fig. 6A). The median survival of patients in the two groups was 443 days (high) and 3,411 days (low) respectively (Fig. 6A, and Additional file 1: Table S8). Notably, increased expression of genes in the molecular group was frequently observed in the same gliomas (Fig. 6B). Approximately 71.92% of gliomas with increased expression of genes in the molecular group had at least two genes with increased expression (Fig. 6B). Among grade II-primary, II-recurrence, III-primary, II-recurrence, IV-primary, IV-recurrence gliomas and IV-secondary gliomas, the total ratio of gene groups with high expression of a single gene was ~24.71%, ~52.50%, ~40.88%, ~58.3%, ~83.98%, ~89.91% and ~100%, respectively (Fig. 6C, and Additional file 1: Table S9), further indicating that activation of the embryonic/

germ cell-like developmental axis may be associated with the pathological grade, recurrence and progression of gliomas. Interestingly, the mRNA profiles of the molecular group could be used to separate poor outcomes from improved outcomes among patients who harboured gliomas with the same WHO grade, especially among the patients with grade III gliomas (Fig. 6C, and Additional file 1: Table S8, S10). Median survival was 344 days (higher) and 710 days (lower) among patients with grade IV gliomas, 544 days (higher) and 2633 days (lower) among patients with grade III gliomas, and 2,219 days (higher) and more than 5,000 days (lower) among patients with grade II gliomas (Fig. 6D, Additional file 1: Fig. S8 and Table S8). Notably, glioma classification based on the WHO grade and molecular group could predict clinical behaviours more accurately (Fig. 6E, Additional file 1: Fig. S9A and Table S8, S10). Subtype grade II gliomas with lower expression of genes in the molecular group had favourable clinical outcomes (Fig. 6D, Additional file 1: Fig. S8, and Table S8). Grade III gliomas with higher expression of genes in the molecular group were similar to grade IV gliomas in terms of clinical outcomes (Fig. 6D, Additional file 1: Fig. S8, and Table S8).

In the revised WHO classification of 2016, combining the IDH and 1p19q status serves as a diagnostic molecular biomarker for gliomas. Then we combining the IDH and 1p19q status subdivided gliomas into three groups, including IDH mutant with 1p19q codeletion, IDH mutant without 1p19q codeletion and IDH wildtype. Among the gliomas with IDH mutant and 1p19q codeletion, IDH mutant and 1p19q non-codeletion as well as IDH wildtype in the combined dataset, the median survival of the three groups of patients was >5000 days, 1258 days and 420 days (Fig. 6E and Additional file 1: Table S11) respectively. Combining the IDH and 1p19q status together with our molecular group could subdivided gliomas into six groups. Among the gliomas with IDH mutant and 1p19q codeletion in the combined dataset, the median survival of the two groups of patients was both >5000 days (Fig. 6F and Additional file 1: Table S8). Among the gliomas with IDH mutant and 1p19q non-codeletion in the combined dataset, the median survival of the two groups of patients was 723 days (higher) and 2552 days (lower) (Fig. 6F and Additional file 1: Table S8) respectively. Among the gliomas with IDH wildtype in the combined dataset, the median survival

(See figure on next page.)

Fig. 4 Association between the embryonic/germ cell related gene expression and outcomes of gliomas. RNA sequencing and clinical data showing the mRNA expression profiles of various genes related to IPS reprogramming (A) and germ cell development and early blastomere formation (B) in gliomas that had different outcomes. C Relationship between the mRNA level of embryonic/germ cell-related genes and overall survival of patients. D The role of the embryonic/germ cell related gene expression in outcomes of gliomas. *P < 0.05, **P < 0.01, ***P < 0.001, ****P < 0.0001

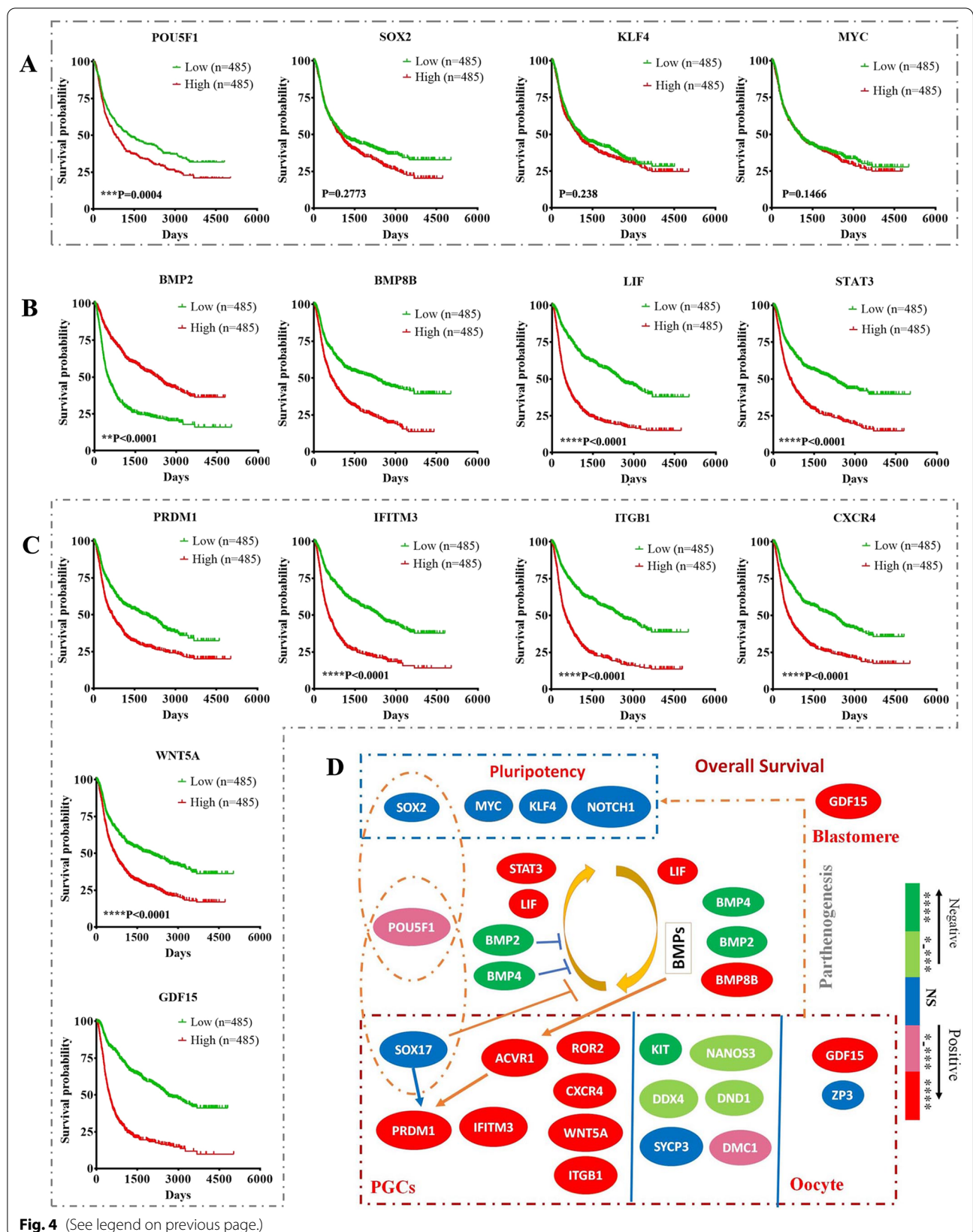
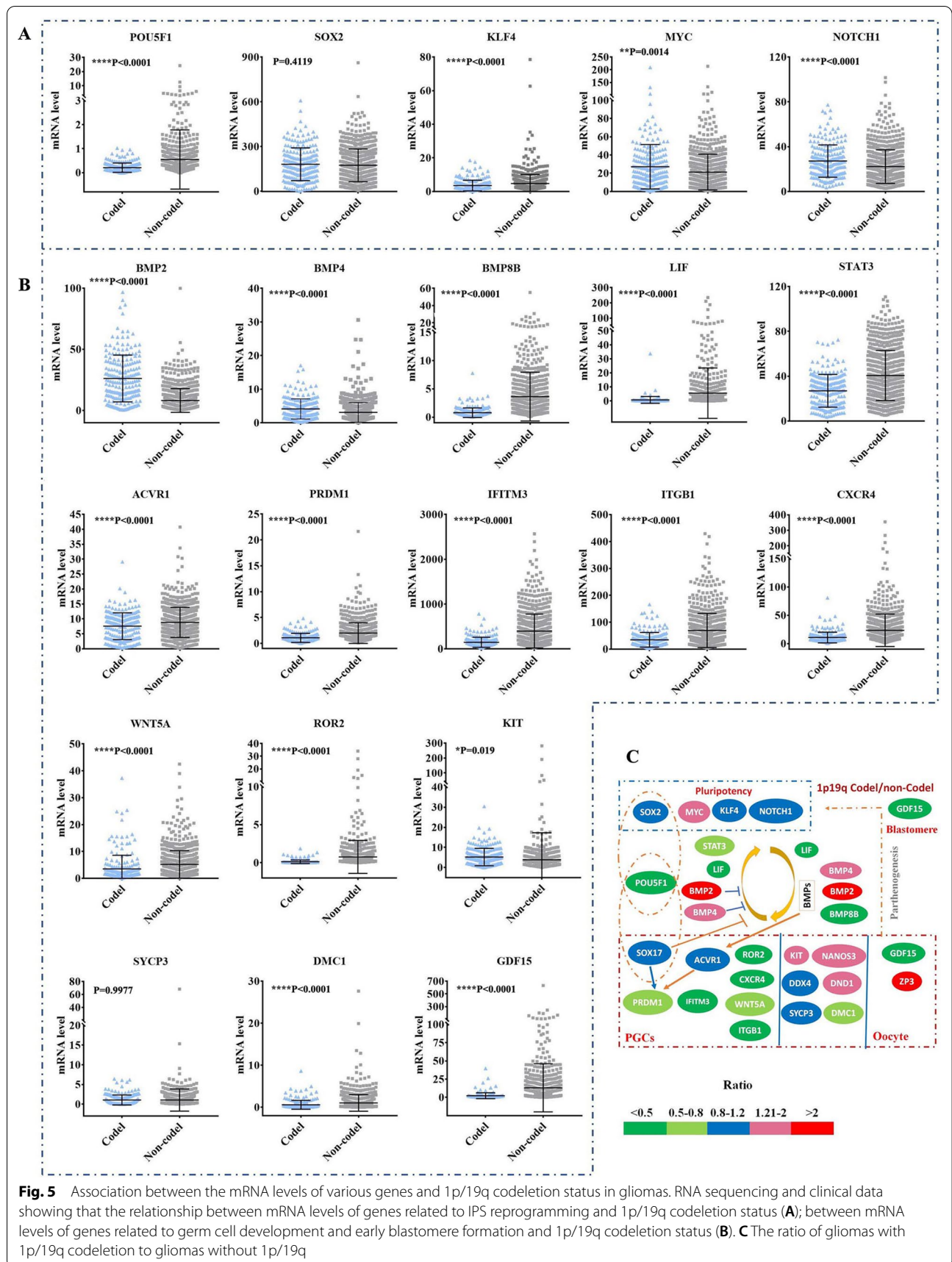


Fig. 4 (See legend on previous page.)



of the two groups of patients was 387 days (higher) and 1196 days (lower) (Fig. 6F and Additional file 1: Table S8) respectively.

We then used 1p19q status together with our molecular group to classified the gliomas. Among patients who had gliomas with 1p19q codeletion in the combined dataset, patients with higher expression of genes in the gene group (median survival=1265 days) had much poorer overall survival than patients with lower expression of genes in the molecular group (median survival >5000 days) (Fig. 6G and Additional file 1: Table S8). Among the gliomas without 1p19q codeletion in the combined dataset, the median survival of the two groups of patients was 415 days (higher) and 2382 days (lower) (Fig. 6H and Additional file 1: Table S8) respectively. Classification by combining the 1p19q status and the molecular group could subdivide gliomas into four subtypes with distinct clinical outcomes (Fig. 6H, and Additional file 1: Table S8), suggesting a possible molecular method to predict clinical behaviour. These findings indicate that the embryonic/germ cell cycle-related molecular group can be used as a good marker for predicting clinical outcomes and may be associated to the low-glioma progression to advanced gliomas.

Appearance of embryonic/germ cell-like cells in gliomas

We then investigated whether embryonic/germ cell-like cells were present in human gliomas and linked to malignant traits. HE and immune staining showed that germ cell-like cells could be observed in some human glioma tissues, and the appearance of germ cell-like cells was associated with the pathological grade of gliomas (Figs. 7 and 8 and Additional file 1: Fig. S9). Compared with LGG, germ cell-like cells were easily observed in GBM (Additional file 1: Table S12). Notably, a series of embryonic/germ cell-like cells at different developmental stages could be observed in the same tumour tissues among some grade IV gliomas (approximately 40%), including PGC-like cells, oocyte-like cells and parthenogenetic preimplantation embryo-like cells, indicating that a somatic parthenogenetic embryo-like cycle might be present in some GBM (Fig. 7B, and Additional file 1: Fig. S9). It was documented that polyploid giant cancer cells (PGCCs) were blastomere-like cells [1, 49]. Taken together, it is

possible that activation of the embryonic/germ cell-like developmental axis occurs during tumour initiation and malignant prognosis.

Discussion

Our findings showed that germ cell-like cells were present in cultured glioma cells and glioma tissues and that deletion of *DAZL* repressed both PGC-like cell formation and tumour initiation in human glioma cell lines. Moreover, the mRNA sequencing results showed that a series of genes related to reprogramming, PGC specification and germ cell development could be detected in most gliomas. Together with reports that embryonic/germ cell-specific genes are essential in malignant tumour behaviours [17–27, 50], it is possible that activation of the embryonic/germ cell-like state may be a necessary precondition for glioma development, which can explain why gliomas show high embryonic/germ cell traits and extensively express genes related to embryonic/germ cell development and testis antigens of tumours [2, 5, 15, 16, 24, 26].

However, our findings indicated that reprogramming activation or germ cell-like state activation alone seemed to be insufficient to lead to a malignant prognosis. In contrast, the increased mRNA levels of genes related to the activation of the embryonic/germ cell-like cycle showed strong correlations with malignant prognoses and poor clinical outcomes, possibly because this cycle could lead to tumours with migratory PGC-like cells (which are linked to metastasis) and a naive ES/PGC-like state (which is linked to tumorigenicity) through the somatic parthenogenetic embryo-like cycle or somatic PGC-EGC-like cycle. Furthermore, committed PGC state which was induced by *DAZL* from migratory PGCs (uncommitted state) was hardly reversed to ES state [34, 35]. Consistent with this, high expression of the genes associated with PGC fate determination usually did not lead to poor outcomes of gliomas, such as *KIT*, *DND1*, *NANOS3* and *DDX4* [34–37]. Notably, it was shown that some core oncogenes/tumour suppressors strongly upregulated/repressed IPS reprogramming (*TP53*, *RB*, *MYC*) [45], PGC-like cell formation (*TP53*), PGC-EGC conversion (*TP53*, *PTEN*) [9], meiosis (*TP53*) [51] and primary oocyte maturation (*TP53*) [20, 52], which further supported the essential role of the embryonic/germ

(See figure on next page.)

Fig. 6 Clinical significance and prevalence of molecular groups among gliomas. **A** Patients separated by the mRNA level of genes in the gene group showed different overall survival. **B** Distribution of gliomas with high expression of single to multiple genes in molecular groups among gliomas with higher expression of genes in molecular groups. **C** Prevalence of the molecular groups among distinct pathological grades. **D** Gliomas classified according to the WHO grade or the WHO combined with the molecular group showed different overall survival. **E** Gliomas classified according to the status of IDH and 1p19q. **F** Patients with the same IDH and 1p19q status classified by the molecular group showed different overall survival. **G** Patients with the same 1p19q status classified by the molecular group showed different overall survival. **H** Gliomas classified according to 1p19q status and the molecular group showed different overall survival

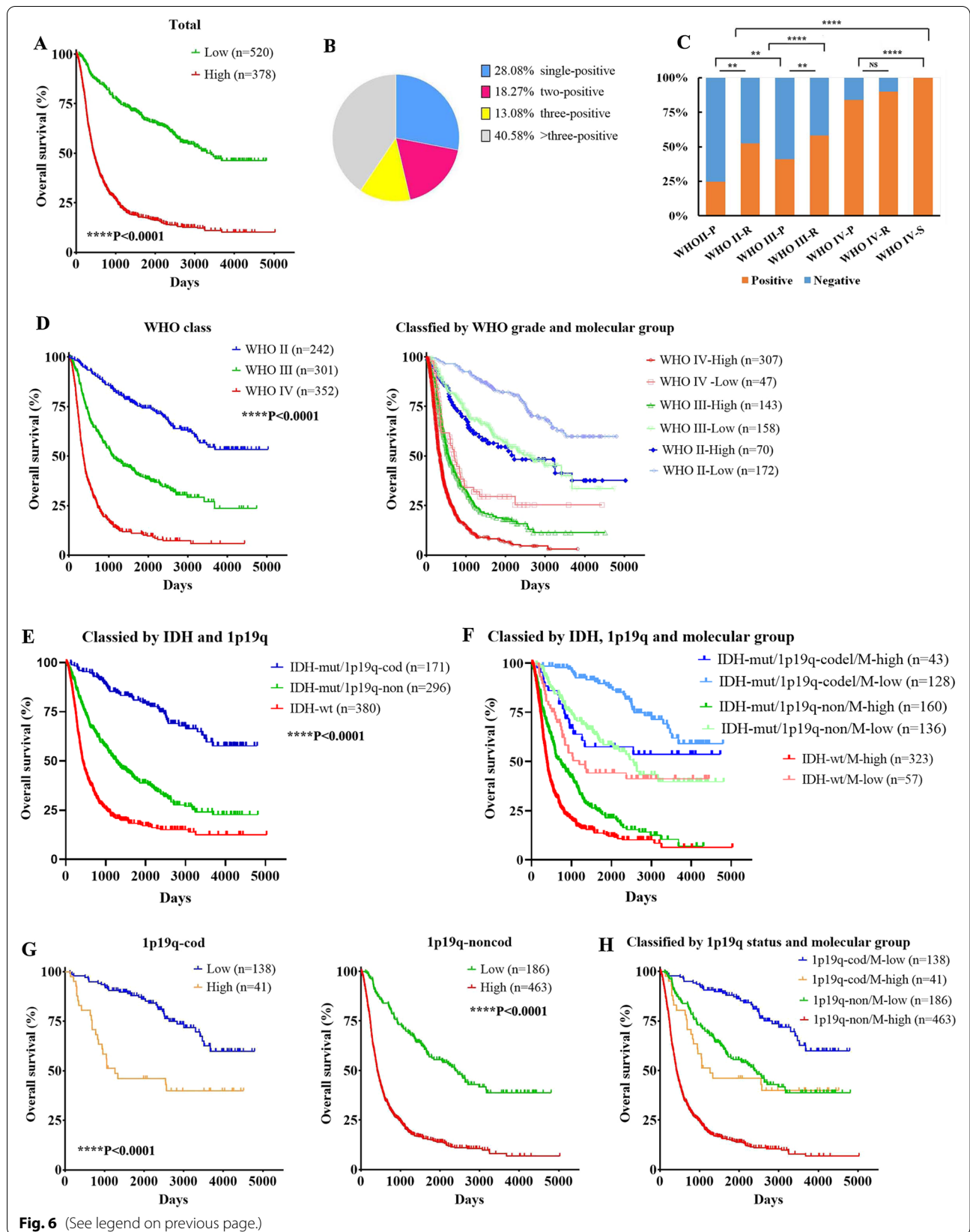


Fig. 6 (See legend on previous page.)

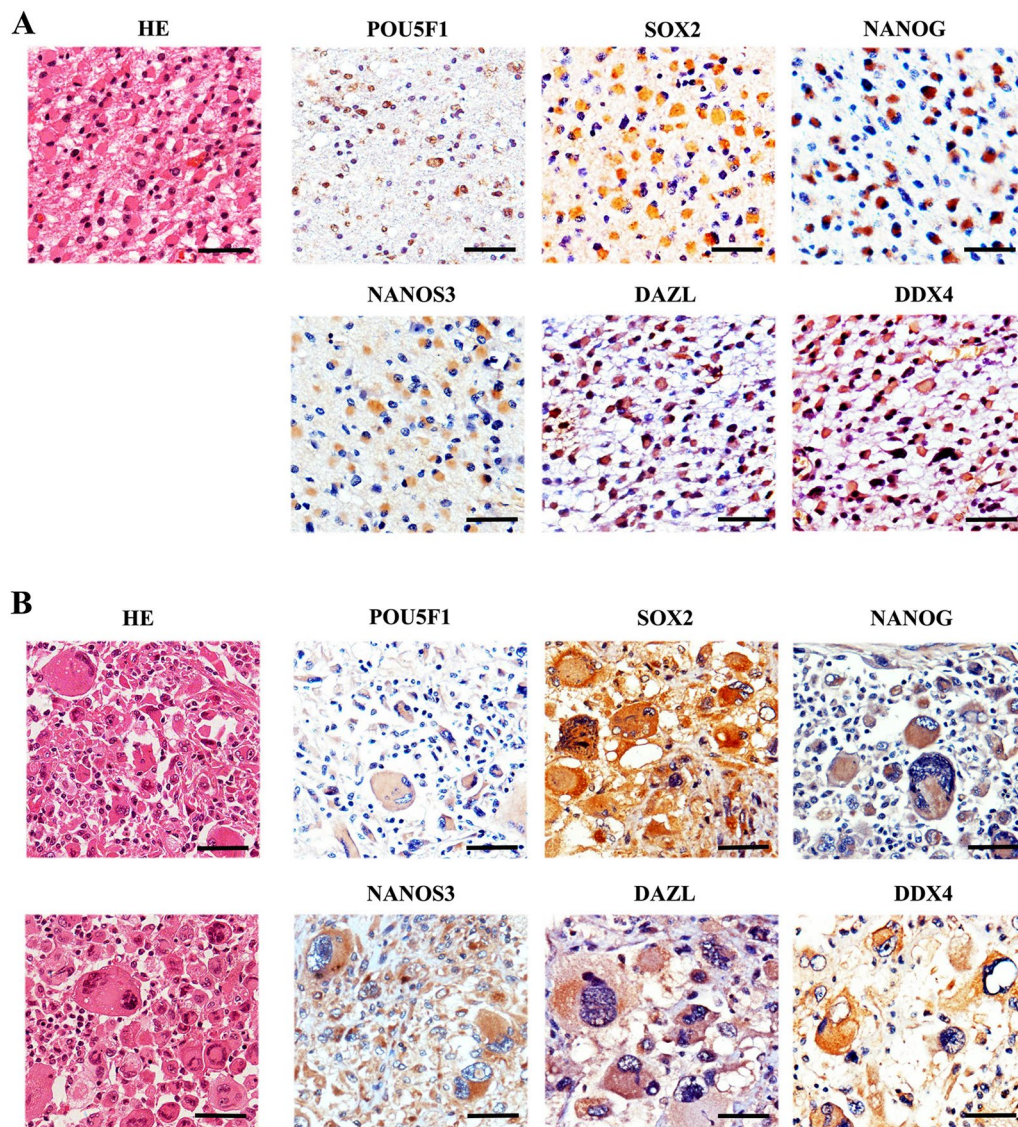


Fig. 7 Appearance of germ cell-like cells in human glioma tissues. **A** Immunohistochemistry assays showing the expression and colocalization of the indicated proteins in lower-grade gliomas. **B** Immunohistochemistry assays showing the expression and colocalization of the indicated proteins in grade IV gliomas. Scale bar = 50 μ m

cell-like cycle in malignant tumour prognosis [53]. The *TP53* or *PTEN* mutation associated with aggressive gliomas were also documented [5, 54–56]. *TP53* or *PTEN* mutation sites could cause different gain/loss of function. Our previous study [20] and some documents showed *TP53* or *PTEN* deletion [9, 45] would promote the embryonic/germ cell-like cell formation. Whether different *TP53* or *PTEN* mutations could cause the similar re-activation of embryonic/germ cell traits is not clear. It will be interesting to explore this possibility in the future.

PGC-like cells and GBM stem-like cell populations might be different but have the intimate link. In fact,

many germ cell markers were used to identify cancer stem cells, such as *SSEA1*, *CD117*, *Sox2*, *PRDM14* [16, 18, 22, 25]. Especially, *SSEA1*, a marker of PGCs, was a general marker of tumour initiating cells in human glioblastoma [16], which provided the close link between GBM stem-like cell populations and PGC-like cells. In our views, the GBM stem-like cells might represent one of status of embryonic/germ cell axis, resembling early PGC-like population. Distinct from cancer stem cell concept, our data indicated that it is possible that the real cancer stemness is not the “cancer stem cells” but the whole embryonic/germ cell-like developmental

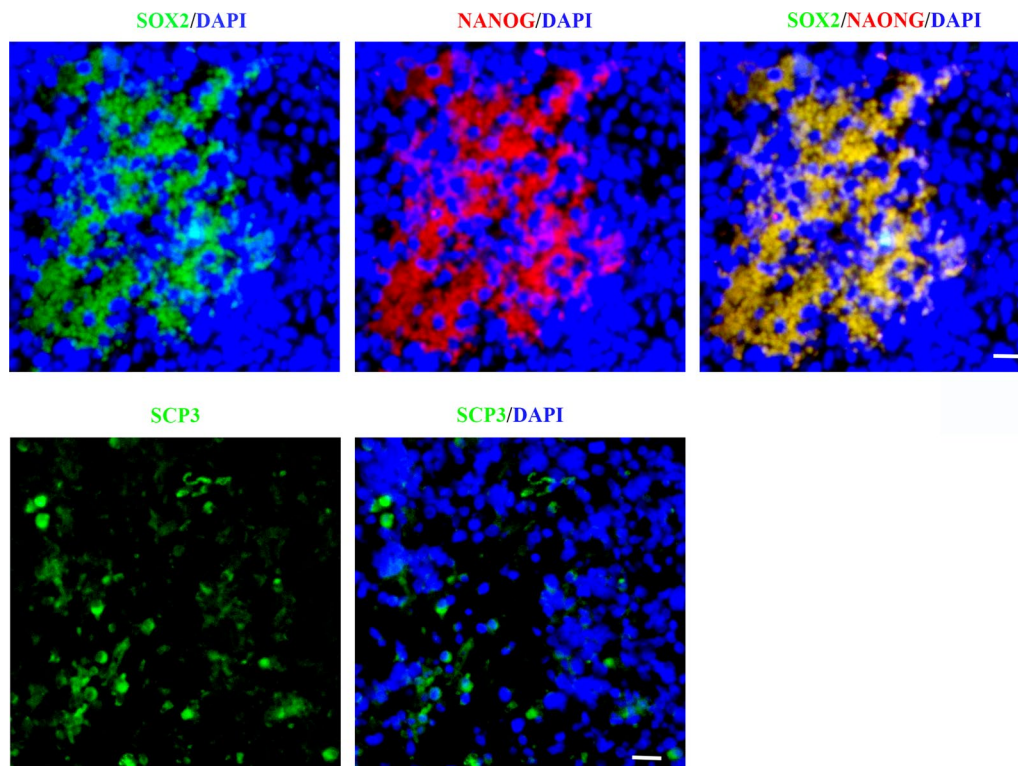


Fig. 8 Immunofluorescence assays of embryonic/germ cell-related protein in human glioma tissues. **A** Co-staining of embryonic/germ cell-related protein in human glioma tissues. **B** Immunofluorescence assays showed the expression of meiosis marker in human glioma tissues. Scale bar = 25 μm

axis including a serial of developmental status, such as embryonic stem-like cells, PGC-like cells, late germ cells and early blastomere-like cells [53].

In summary, our findings indicated that a crucial role of germ cell-like cell formation in glioma initiation as well as activation of the parthenogenetic embryo-like cycle and PGC-EGC-like cycle might represent two driving events in the malignant prognosis of gliomas, which may provide a novel way to better understand the nature of glioma and develop targeted therapies for gliomas as well as important markers for predicting clinical outcomes in gliomas.

Abbreviations

CGGA: Chinese Glioblastoma Genome Atlas; EC cells: Embryonal carcinoma cells; EC cells: Embryonal carcinoma cells; EGCs: Embryonic germ cells; ES cells: Embryonic stem cells; iPS cells: Induced pluripotent stem cells; PGCs: Primordial germ cells; GTEx: The Genotype-Tissue Expression; TCGA: The Cancer Genome Atlas; PRDM14: PR/SET Domain 14; PRDM1: PR/SET Domain 1; POU5F1: POU Class 5 Homeobox 1; SOX2: SRY-Box Transcription Factor 2; NANOG: Nanog Homeobox; DAZL: Deleted in Azoospermia Like; DDX4: DEAD-Box Helicase 4; MYC: MYC Proto-Oncogene; BHLH: Transcription factor; KLF4: KLF Transcription Factor 4; NOTCH1: Notch Receptor 1; BMP2: Bone Morphogenetic Protein 2; BMP4: Bone Morphogenetic Protein 4; BMP8B: Bone Morphogenetic Protein 8b; LIF: LIF Interleukin 6 Family Cytokine; SOX17: SRY-Box Transcription Factor 17; ACVR1: Activin A Receptor Type 1; IFITM3: Interferon Induced Transmembrane Protein 3; KIT: KIT Proto-Oncogene,

Receptor Tyrosine Kinase; NANOS3: Nanos C2HC-Type Zinc Finger 3; DND1: DND MicroRNA-Mediated Repression Inhibitor 1; ITGB1: Integrin Subunit Beta 1; CXCR4: C-X-C Motif Chemokine Receptor 4; WNT5A: Wnt Family Member 5 A; ROR2: Receptor tyrosine kinase like orphan receptor 2; SYCP3: Synaptonemal Complex Protein 3; DMC1: DNA Meiotic Recombinase 1; TP53: Tumor Protein P53; PTEN: Phosphatase And Tensin Homolog; STAT3: Signal transducer and activator of transcription 3; ZP3: Zona Pellucida Glycoprotein 3; GDF15: Growth differentiation factor 15.

Supplementary Information

The online version contains supplementary material available at <https://doi.org/10.1186/s12935-022-02792-8>.

Additional file 1: Figure S1. PCR showed the DAZL with heterozygote (arrow). **Figure S2.** (A) Immunofluorescence assays showed the expression of DAZL in cultured A172^{mut} cells. (B) AP staining showing PGC-like cells in A172^{mut} glioma cells. (C) The comparison of indicated genes between A172 bottom cells and A172 upper cells. Scale bar = 25 μm . **Figure S3.** Increase expression of genes related to embryonic/germ cell development in gliomas versus normal brain tissues. * $P < 0.01$. **Figure S4.** Association between the expression of genes related to embryonic/germ cell development and the pathologic grades/outcomes of gliomas. (A) RNA sequencing showing the mRNA expression profiles of the indicated genes in subtypes of gliomas that had different pathologic grades. (B) RNA array showing the mRNA expression profile of DAZL in subtypes of gliomas that had different pathologic grades. **Figure S5.** Association between the expression of genes related to embryonic/germ cell development and the pathologic grades/outcomes of gliomas. (A) RNA sequencing and clinical data showing the mRNA expression profiles of the genes related to IPS reprogramming in gliomas that had different pathologic grades and

outcomes. (B) RNA sequencing and clinical data showing the mRNA expression profiles of the genes related to IPS reprogramming in gliomas that had different pathologic grades and outcomes. (C) RNA array showing the mRNA expression profile of DAZL in gliomas that had different pathologic grades. **Figure S6.** Association between the expression of genes related to pluripotency and the pathologic grades/outcomes of gliomas. (A) RNA sequencing and clinical data showing the mRNA expression profiles of the indicated genes in gliomas that had different pathologic grades and outcomes. **Figure S7.** Association between the mRNA levels of various genes and 1p/19q codeletion status in gliomas. (A) RNA sequencing and clinical data showing the relationship between the mRNA level of the indicated genes and 1p/19q codeletion status. (B) The ratio of gliomas with 1p/19q codeletion to gliomas without 1p/19q codeletion and the mean mRNA values of various genes. **Figure S8.** Clinical significance and prevalence of molecular groups among gliomas. (A) Patients with the same pathological grade separated by the mRNA level of genes in the gene group showed different overall survival. **Figure S9.** Appearance of germ cell-like cells in human glioma tissues. (A) Morphology and marker expression of embryonic/germ cell-like cells in human glioma tissues. (B) HE staining and Immunohistochemistry assays showing the germ cell-like cell and embryonic structures at different developmental stages. **Table S1.** Sequencing data of CRISPR-Cas9 knockout glioma cells. **Table S2.** Detailed information from the CGGA database regarding mRNA sequencing. **Table S3.** Comparison of gene expression in subtype of gliomas with distinct WHO classification (Unpaired t test with Welch's correction). **Table S4.** Comparison of gene expression in gliomas with distinct WHO classifications (Unpaired t test with Welch's correction and Mann-Whitney test). **Table S5.** Comparison of the median survival of gliomas with distinct gene expression. **Table S6.** Comparison of gene expression in gliomas with distinct 1p/19q codeletion status (Unpaired t test with Welch's correction). **Table S7.** RNA sequencing cut-off values of the genes in the molecular group. **Table S8.** Comparison of the median survival of gliomas with distinct classifications. **Table S9.** Positive ratio of molecular groups in distinct glioma types. **Table S10.** Comparison of the median survival of gliomas with the WHO classification. **Table S11.** Comparison of the median survival of gliomas with the WHO classification. **Table S12.** Expression ratio of proteins related to embryonic/germ cells in glioma tissues.

Acknowledgements

The genetic analysis and clinical outcome results are based on data generated from the Chinese Glioma Genome Atlas (CGGA) (<http://cgga.org.cn/index.jsp>), the Cancer Genome Atlas (TCGA) and the Genotype-Tissue Expression (GTEx). Some data were analysed using the <http://gepia2.cancer-pku.cn/#analysis>.

Author contributions

ZM, and ZF performed the experiments and analysed the data from the Chinese Glioma Genome Atlas (CGGA). JX performed the immunofluorescence assays. HZ provided the glioma tissues and pathologic information. HKL provided some advice. CL designed the experiments, analysed the data and wrote the paper. All the authors read and approved the final manuscript.

Funding

This work was supported by the Natural Science Foundation of Shanghai (21ZR1410900), the Natural Science Foundation of China (No. 82273113) and Shanghai Municipal Key Clinical Specialty of China (shslczdzk03303).

Availability of data and materials

The authors confirm that the data supporting the findings of this study are available within the article and its additional materials.

Declarations

Ethics approval and consent to participate

The study protocol was approved by the Medical Ethics Committee of Huashan Hospital, Fudan University (permit number MEC-HS (Hu) 2011 – 362), and informed consent was obtained from each patient. All research was performed in accordance with relevant guidelines and regulations. Our study was carried out in compliance with the American Veterinary Medical Association

(AVMA) Guidelines for the Euthanasia of Animals (2020). All animal protocols were carried out in accordance with ARRIVE guidelines. All animal experiments were approved by with the Institutional Animal Care and Use Committee of Fudan University (approval number: 2019JS-073).

Consent for publication

All authors read and approved the final manuscript.

Competing interests

The authors declare that they have no conflicts of interest.

Author details

¹Department of Laboratory Medicine, Shanghai Medical College, Huashan Hospital, Fudan University, Shanghai 200040, China. ²Department of Laboratory Medicine, Shanghai Children's Hospital, Shanghai Jiao Tong University, Shanghai 200040, China. ³Department of Pathology, Shanghai Medical College, Fudan University, Shanghai 200040, China. ⁴Department of Neurosurgery, Huashan Hospital, Fudan University, Shanghai 200040, China. ⁵Department of Cancer Biology, Wake Forest School of Medicine, Winston-Salem, NC 27157, USA.

Received: 3 February 2022 Accepted: 14 November 2022

Published online: 26 November 2022

References

- Niu N, Mercado-Urbe I, Liu J. Dedifferentiation into blastomere-like cancer stem cells via formation of polyploid giant cancer cells. *Oncogene*. 2017;36(34):4887–900.
- Simpson AJ, Caballero OL, Jungbluth A, Chen YT, Old LJ. Cancer/testis antigens, gametogenesis and cancer. *Nat Rev Cancer*. 2005;5(8):615–25.
- Brewer BG, Mitchell RA, Harandi A, Eaton JW. Embryonic vaccines against cancer: an early history. *Exp Mol Pathol*. 2009;86(3):192–7.
- Bignold LP, Coghlan BL, Jersmann HP, Hansemann, Boveri, chromosomes and the gametogenesis-related theories of tumours. *Cell Biol Int*. 2006;30(7):640–4.
- Old LJ. Cancer/testis (CT) antigens—a new link between gametogenesis and cancer. *Cancer Immun*. 2001;1:1.
- Stevens LC. Origin of testicular teratomas from primordial germ cells in mice. *J Natl Cancer Inst*. 1967;38(4):549–52.
- Stevens LC. The development of transplantable teratocarcinomas from intratesticular grafts of pre- and postimplantation mouse embryos. *Dev Biol*. 1970;21(3):364–82.
- Stevens LC, Little CC. Spontaneous testicular teratomas in an inbred strain of mice. *Proc Natl Acad Sci U S A*. 1954;40(11):1080–7.
- Kimura T, Suzuki A, Fujita Y, Yomogida K, Lomeli H, Asada N, Ikeuchi M, Nagy A, Mak TW, Nakano T. Conditional loss of PTEN leads to testicular teratoma and enhances embryonic germ cell production. *Development*. 2003;130(8):1691–700.
- Thomson JA, Itskovitz-Eldor J, Shapiro SS, Waknitz MA, Swiergiel JJ, Marshall VS, Jones JM. Embryonic stem cell lines derived from human blastocysts. *Science*. 1998;282(5391):1145–7.
- Takahashi K, Tanabe K, Ohnuki M, Narita M, Ichisaka T, Tomoda K, Yamanaka S. Induction of pluripotent stem cells from adult human fibroblasts by defined factors. *Cell*. 2007;131(5):861–72.
- Ben-Porath I, Thomson MW, Carey VJ, Ge R, Bell GW, Regev A, Weinberg RA. An embryonic stem cell-like gene expression signature in poorly differentiated aggressive human tumors. *Nat Genet*. 2008;40(5):499–507.
- Ezeh UI, Turek PJ, Reijo RA, Clark AT. Human embryonic stem cell genes OCT4, NANOG, STELLAR, and GDF3 are expressed in both seminoma and breast carcinoma. *Cancer*. 2005;104(10):2255–65.
- Rudin CM, Durinck S, Stawiski EW, Poirier JT, Modrusan Z, Shames DS, Bergbower EA, Guan Y, Shin J, Guillory J, et al. Comprehensive genomic analysis identifies SOX2 as a frequently amplified gene in small-cell lung cancer. *Nat Genet*. 2012;44(10):1111–6.
- Guo Y, Liu S, Wang P, Zhao S, Wang F, Bing L, Zhang Y, Ling EA, Gao J, Hao A. Expression profile of embryonic stem cell-associated genes Oct4, Sox2 and nanog in human gliomas. *Histopathology*. 2011;59(4):763–75.

16. Son MJ, Woolard K, Nam DH, Lee J, Fine HA. SSEA-1 is an enrichment marker for tumor-initiating cells in human glioblastoma. *Cell Stem Cell*. 2009;4(5):440–52.
17. Mu P, Zhang Z, Benelli M, Karthaus WR, Hoover E, Chen CC, Wongvipat J, Ku SY, Gao D, Cao Z, et al. SOX2 promotes lineage plasticity and antiandrogen resistance in TP53- and RB1-deficient prostate cancer. *Science*. 2017;355(6320):84–8.
18. Boumahdi S, Driessens G, Lapouge G, Rorive S, Nassar D, Le Mercier M, Delatte B, Caauwe A, Lenglez S, Nkusi E, et al. SOX2 controls tumour initiation and cancer stem-cell functions in squamous-cell carcinoma. *Nature*. 2014;511(7508):246–50.
19. Liu C, Ma Z, Hou J, Zhang H, Liu R, Wu W, Liu W, Lu Y. Germline traits of human hepatoblastoma cells associated with growth and metastasis. *Biochem Biophys Res Commun*. 2013;437(1):120–6.
20. Liu C, Cai Z, Jin G, Peng D, Pan BS, Zhang X, Han F, Xu X, Lin HK. Abnormal gametogenesis induced by p53 deficiency promotes tumor progression and drug resistance. *Cell Discov*. 2018;4:54.
21. Liu C, Ma Z, Cai Z, Zhang F, Liu C, Chen T, Peng D, Xu X, Lin HK. Identification of primordial germ cell-like cells as liver metastasis initiating cells in mouse tumour models. *Cell Discov*. 2020;6:15.
22. Moriya C, Taniguchi H, Miyata K, Nishiyama N, Kataoka K, Imai K. Inhibition of PRDM14 expression in pancreatic cancer suppresses cancer stem-like properties and liver metastasis in mice. *Carcinogenesis*. 2017;38(6):638–48.
23. Chen CL, Uthaya Kumar DB, Punj V, Xu J, Sher L, Tahara SM, Hess S, Machida K. NANOG metabolically reprograms tumor-initiating stem-like cells through tumorigenic changes in oxidative phosphorylation and fatty acid metabolism. *Cell Metab*. 2016;23(1):206–19.
24. Zhang F, Liu R, Zhang H, Liu C, Liu C, Lu Y. Suppressing Dazl modulates tumorigenicity and stemness in human glioblastoma cells. *BMC Cancer*. 2020;20(1):673.
25. Adhikari AS, Agarwal N, Wood BM, Porretta C, Ruiz B, Pochampally RR, Iwakuma T. CD117 and Stro-1 identify osteosarcoma tumor-initiating cells associated with metastasis and drug resistance. *Cancer Res*. 2010;70(11):4602–12.
26. Janic A, Mendizabal L, Llamazares S, Rossell D, Gonzalez C. Ectopic expression of germline genes drives malignant brain tumor growth in *Drosophila*. *Science*. 2010;330(6012):1824–7.
27. Kaufman CK, Mosimann C, Fan ZP, Yang S, Thomas AJ, Ablain J, Tan JL, Fogley RD, van Rooijen E, Hagedorn EJ, et al. A zebrafish melanoma model reveals emergence of neural crest identity during melanoma initiation. *Science*. 2016;351(6272):aad2197.
28. Liu C, Ma Z, Xu S, Hou J, Hu Y, Yu Y, Liu R, Chen Z, Lu Y. Activation of the germ-cell potential of human bone marrow-derived cells by a chemical carcinogen. *Sci Rep*. 2014;4:5564.
29. Liu C, Xu S, Ma Z, Zeng Y, Chen Z, Lu Y. Generation of pluripotent cancer-initiating cells from transformed bone marrow-derived cells. *Cancer Lett*. 2011;303(2):140–9.
30. Ma Z, Hu Y, Jiang G, Hou J, Liu R, Lu Y, Liu C. Spontaneous generation of germline characteristics in mouse fibrosarcoma cells. *Sci Rep*. 2012;2:743.
31. Ma Z, Liu R, Wang X, Huang M, Gao Q, Lu Y, Liu C. Spontaneous germline potential of human hepatic cell line in vitro. *Mol Hum Reprod*. 2013;19(4):216–26.
32. Donehower LA, Harvey M, Slagle BL, McArthur MJ, Montgomery CA Jr, Butel JS, Bradley A. Mice deficient for p53 are developmentally normal but susceptible to spontaneous tumours. *Nature*. 1992;356(6366):215–21.
33. Oosterhuis JW, Looijenga LHJ. Human germ cell tumours from a developmental perspective. *Nat Rev Cancer*. 2019;19(9):522–37.
34. Nicholls PK, Schorle H, Naqvi S, Hu YC, Fan Y, Carmell MA, Dobrinski I, Watson AL, Carlson DF, Fahrenkrug SC, et al. Mammalian germ cells are determined after PGC colonization of the nascent gonad. *Proc Natl Acad Sci U S A*. 2019;116(51):25677–87.
35. Mikedis MM, Fan Y, Nicholls PK, Endo T, Jackson EK, Cobb SA, de Rooij DG, Page DC. DAZL mediates a broad translational program regulating expansion and differentiation of spermatogonial progenitors. *Elife*. 2020;9:e56523.
36. Saitou M, Yamaji M. Primordial germ cells in mice. *Cold Spring Harb Perspect Biol*. 2012;4(11):a008375.
37. Strome S, Updike D. Specifying and protecting germ cell fate. *Nat Rev Mol Cell Biol*. 2015;16(7):406–16.
38. Tang WW, Kobayashi T, Irie N, Dietmann S, Surani MA. Specification and epigenetic programming of the human germ line. *Nat Rev Genet*. 2016;17(10):585–600.
39. Fukunaga N, Teramura T, Onodera Y, Takehara T, Fukuda K, Hosoi Y. Leukemia inhibitory factor (LIF) enhances germ cell differentiation from primate embryonic stem cells. *Cell Reprogram*. 2010;12(4):369–76.
40. Tarone G, Russo MA, Hirsch E, Odoriso T, Altruda F, Silengo L, Siracusa G. Expression of beta 1 integrin complexes on the surface of unfertilized mouse oocyte. *Development*. 1993;117(4):1369–75.
41. Anderson R, Fassler R, Georges-Labouesse E, Hynes RO, Bader BL, Kreidberg JA, Schaible K, Heasman J, Wylie C. Mouse primordial germ cells lacking beta1 integrins enter the germline but fail to migrate normally to the gonads. *Development*. 1999;126(8):1655–64.
42. Makoolati Z, Movahedin M, Forouzandeh-Moghadam M. In vitro germ cell differentiation from embryonic stem cells of mice: induction control by BMP4 signalling. *Biosci Rep*. 2016;36(6):e00407.
43. Zdravkovic T, Nazor KL, Larocque N, Gormley M, Donne M, Hunkapillar N, Giritharan G, Bernstein HS, Wei G, Hebrok M, et al. Human stem cells from single blastomeres reveal pathways of embryonic or trophoblast fate specification. *Development*. 2015;142(23):4010–25.
44. Soucek K, Malenovska A, Kahounova Z, Remsik J, Holubcova Z, Soukup T, Kurfurstova D, Bouchal J, Suchankova T, Slabakova E, et al. Presence of growth/differentiation factor-15 cytokine in human follicular fluid, granulosa cells, and oocytes. *J Assist Reprod Genet*. 2018;35(8):1407–17.
45. Kawamura T, Suzuki J, Wang YV, Menendez S, Morera LB, Raya A, Wahl GM, Belmonte JC. Linking the p53 tumour suppressor pathway to somatic cell reprogramming. *Nature*. 2009;460(7259):1140–4.
46. Yamada Y, Davis KD, Coffman CR. Programmed cell death of primordial germ cells in *Drosophila* is regulated by p53 and the Outsiders monocarboxylate transporter. *Development*. 2008;135(2):207–16.
47. Cancer Genome Atlas, Research N, Brat DJ, Verhaak RG, Aldape KD, Yung WK, Salama SR, Cooper LA, Rheinbay E, Miller CR, Vitucci M, et al. Comprehensive, integrative genomic analysis of diffuse lower-grade gliomas. *N Engl J Med*. 2015;372(26):2481–98.
48. Ohgaki H, Kleihues P. The definition of primary and secondary glioblastoma. *Clin Cancer Res*. 2013;19(4):764–72.
49. Liu J. The “life code”: a theory that unifies the human life cycle and the origin of human tumors. *Semin Cancer Biol*. 2020;60:380–97.
50. Liu X, Chen L, Fan Y, Hong Y, Yang X, Li Y, Lu J, Lv J, Pan X, Qu F, et al. IFITM3 promotes bone metastasis of prostate cancer cells by mediating activation of the TGF-beta signaling pathway. *Cell Death Dis*. 2019;10(7):517.
51. Habu T, Wakabayashi N, Yoshida K, Yomogida K, Nishimune Y, Morita T. p53 protein interacts specifically with the meiosis-specific mammalian RecA-like protein DMC1 in meiosis. *Carcinogenesis*. 2004;25(6):889–93.
52. Bolcun-Filas E, Rinaldi VD, White ME, Schimenti JC. Reversal of female infertility by Chk2 ablation reveals the oocyte DNA damage checkpoint pathway. *Science*. 2014;343(6170):533–6.
53. Liu C, Moten A, Ma Z, Lin HK. The foundational framework of tumors: Gametogenesis, p53, and cancer. *Semin Cancer Biol*. 2021. <https://doi.org/10.1016/j.semcancer.2021.04.018>.
54. Jin Y, Xiao W, Song T, Feng G, Dai Z. Expression and prognostic significance of p53 in glioma patients: a meta-analysis. *Neurochem Res*. 2016;41(7):1723–31.
55. Friedmann-Morvinski D, Bushong EA, Ke E, Soda Y, Marumoto T, Singer O, Ellisman MH, Verma IM. Dedifferentiation of neurons and astrocytes by oncogenes can induce gliomas in mice. *Science*. 2012;338(6110):1080–4.
56. Patnam S, Samal R, Koyyada R, Joshi P, Singh AD, Nagalla B, Soma MR, Sanareddy RR, Ippili K, Raju S, et al. Exosomal PTEN as a predictive marker of aggressive gliomas. *Neurol India*. 2022;70(1):215–22.

Publisher's Note

Springer Nature remains neutral with regard to jurisdictional claims in published maps and institutional affiliations.